Journal: ACP
Title: Chemical characterization and source apportionment of submicron aerosols measured in Senegal during the 2015 SHADOW campaign
Author(s): Laura-Hélèna Rivellini et al.
MS No.: acp-2016-1127

The authors want to thank Reviewer #2 for his/her helpful comments. They are addressed below in blue. Changes in the manuscript are written in red.

Anonymous Referee #2

1. Please consider revising the calculated Fe concentrations and/or the PM1 concentrations and/or the ACSM concentrations (RF for NO3). These data together have inconsistencies that need to be addressed or commented and the possible sources of uncertainty should be stated. The authors report a mean value of 4.6% for the Fe/PM1 ratio. This means 16% for the Fe/RefractoryPM1, since 71% of PM_1 is NR-PM1. (Or 20% for the ratio Fe/(PM1-ACSM-BC) according to Figure S2, considering 5% of Fe and 25% of PM1-ACSM-BC). Hence, it is this 16% (or 20%) which should be compared to the data in the literature, given that the literature data that the authors quote make reference to Dust (and not total PM, regardless of the size fraction). Please see some additional comments related to this one below.

Author's response:
The reviewer is correct in stating that comparison to literature data should be made considering the iron content in dust (and not in total PM_1). The dust amount in our case corresponds to the sum of the unaccounted fraction (assuming negligible influence of sea salt), and Fe obtained by deconvolving absorption measurements, that is to say 25% (Figure S2). The Fe/(Fe + Unacc.) ratio is therefore 20% on average (varying between 12% for marine and 23% for continental days on average, Figures R1a-c).
Table R1 below summarizes the iron content determined in Saharan samples, which shows that the relative contribution of iron determined in this work is in the same order of magnitude but still significantly higher. However iron oxides can be found mostly (for ~2/3) in the clay fraction (~$PM_{2.5}$) and ~1/3 in the silt (coarse) fraction (Journet et al., 2014; Kandler et al., 2009), which is consistent with increased ratios in the submicron fraction compared to larger ones. It is also worth noting that Val et al. (2013) measured the iron content in the ultrafine and fine fractions (corresponding to PM_1) of particles collected in Dakar, and measured a ratio in the upper range of those already reported in the literature, even in the absence of dust event.

Table R1. Comparison of iron content (in %) determined in Saharan dust and soil samples

Reference	Location	Method [a]	Size fraction	%Fe [b]
Dust samples				
(Lafon et al., 2004)	Banizoumbou (Niger)	XRF; CBD	TSP	6.3; 7.8
(Lafon et al., 2006)	Banizoumbou,	XRF; CBD	TSP	4.3 – 6.1
(Lafon et al., 2006)	Cape Verde	XRF; CBD	TSP	5.3 – 6.0
(Formenti et al., 2008)	Banizoumbou	CBD	40 µm	5.8
(Val et al., 2013)	Dakar (Senegal)	ICP-MS	1 µm	7.8
This work	M'Bour	cf. text	1 µm	23 (continental) 21 (sea breeze) 16 (marine)
Soil samples				
(Moreno et al., 2006)	Saharan region (9 samples)	ICP-AES/ ICP-MS	TSP	2.0 – 4.7
(Lafon et al., 2006)	Banizoumbou,	XRF; CBD	10.2 µm [*] 2.5 µm [*]	5.3 5.8
(Joshi et al., 2017)	M'Bour, Bordj (Algeria), Nefta (Tunisia)	XRD	100 µm	< 0.5

[a] XRF: X-ray Fluorescence (XRF) Spectrometry for elemental analysis; CBD: chemical method based on citrate-bicarbonate-dithionite (CBD) reagent for quantification of iron oxides adapted from soil analysis (Mehra and Jackson, 1960)

[b] Percentages of iron relative to the mass of all oxides, classically taking into account Na_2O, MgO, Al_2O_3, SiO_2, K_2O, CaO, TiO_2 and Fe_2O_3.

[*] Soil samples resuspended using wind tunnel and collected with a 13-stage impactor

The uncertainties in the calculation of the Fe/(Fe + Unacc.) ratio can come from the measurements themselves (those for the ACSM, in particular regarding RF(NO_3), are detailed in the reply to comment 4 and will influence the determination of the unaccounted fraction); but are mostly related to the BC and dust absorption Angström exponents (AAE) corresponding to α and β values, respectively, in the deconvolution method. This method is indeed highly sensitive to even small variations of these parameters, with values quite well known for BC from fossil fuel ranging from 0.8 to 1.1 (Hansen, 2005; Zotter et al., 2017) but not so much for dust. In the manuscript, we chose to use β = - 4, according to Fialho et al. (2006) values determined at the Azores Islands for samples influenced by Saharan dust events. But other values can be found in the literature (Table R2), ranging from -1.6 to -6.5 and largely influenced by the wavelength range as well as dust origins and size fractions since the iron content differ depending on emission sources and particle size (Journet et al., 2014). Even during the SAMUM campaign (May to June 2006 in Morocco), a wide range of AAE values have been reported from 1.6 up to 5.1 for ground-based measurements in the same size fraction, as shown in Table R2.

Table R2. Mineral dust AAE values reported from field campaigns around the Saharan region.

Reference	Location / Period	Wavelengths (nm)	Fraction	β
Fialho et al. (2006) [a]	Azores Islands Jul. 2001 – Jun. 2005	370-950	-	-4
Müller et al. (2009) [a]	Tinfou, Morocco (SAMUM) Summer 2006	467/660	PM_{10}	-2.25 to -5.13
Petzold et al. (2009) [b]	South-East Morocco (SAMUM) Summer 2006	467/660	$PM_{2.5}$	-2 to -6.5
Schladitz et al. (2009) [a]	Tinfou, Morocco (SAMUM) Summer 2006	537/637	PM_{10}	-1.6 to -4.73
(Linke et al., 2006) [c]	Morocco Egypt	266/532	~PM_4	-4.2 -5.3
(Caponi et al., 2017) [c]	Morocco Lybia Algeria Mali	375-850 375-532 375-850 375-532	$PM_{2.5}$ ($PM_{10.6}$)	-2.6 -4.1 (-3.2) -2.8 (-2.5) -3.4

[a] In situ ground-based measurements; [b] Airborne measurements through dust plumes; [c] Laboratory experiments with resuspended soil samples

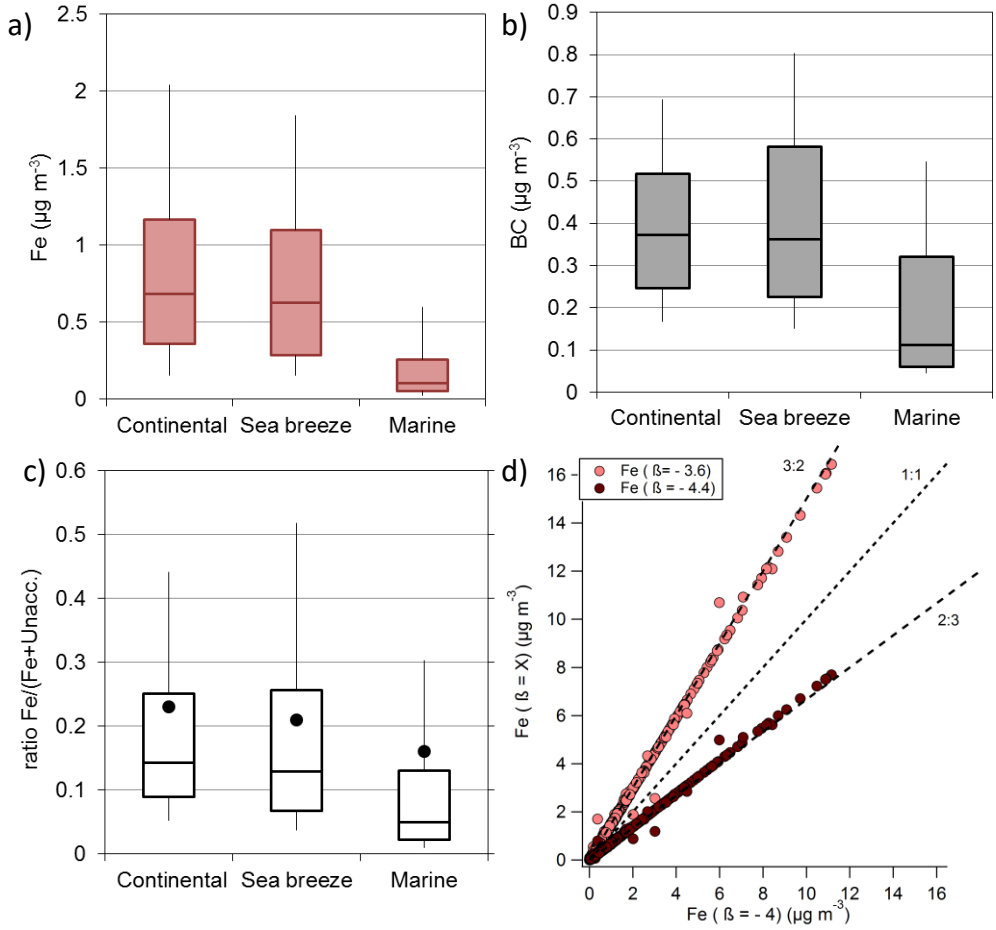

Figure R1. Box plots of (a) Fe, (b) BC concentrations and (c) Fe/(Fe+Unacc.) ratio for continental, sea breeze and marine days. (d) Scatter plot of iron concentrations (in µg m^{-3}) obtained from Fialho's deconvolution method using an AAE value of ± 10% compared to the one from the literature and used in the manuscript.

Applying a relatively small increase (resp. decrease) of 10% on the value of β for our dataset led to a 33% decrease (resp. 50% increase) of iron concentrations, as shown in Figure R1d, but no change in the temporal behavior.

In conclusion, the approach used here leads to an estimate of the absolute concentrations of iron, although with high uncertainties given all the necessary assumptions and the empirical algorithm used to deconvolve BC and Fe from absorption measurements. However the temporal profiles, non-parametric wind regression (NWR) plots and potential source contribution function (PSCF) maps (now provided in Figures S5b and S5c, respectively) are all consistent with the expected behavior of such a desert dust tracer and show that it can be useful in determining the contribution of dust to absorption measurements (see also reply to comment 24). We nonetheless agree with reviewer #2 that there is quite some room for improvement, in particular for a better estimation of the AAE value for dust similar to the efforts carried out to determine the AAE values for BC from fossil fuel and wood burning (Zotter et al., 2017). We strongly believe the lack of information for submicron particles in terms of chemical composition of refractory species and optical properties should be better addressed, but is beyond the scope of this work.

Changes in manuscript:
A new appendix (S2) in the Supplementary Information now includes the whole discussion above. Changes in the main text have been also done page 8, line 18 with a new sentence added: "Applying the propagation for uncertainties approach on the values of K_{Fe} (10%) and the slope b (39%, calculated using a variability of 0.2 for α and β (Fialho et al., 2006)) gives an overall uncertainty of ~40% for iron concentrations. However the deconvolution algorithm is highly sensitive to the values of the Angström absorption exponents (α and β) and a more detailed discussion can be found in Appendix S2."

2. The sampling period is actually 3 months (20 March to 22 June), and not 4 as stated.

Author's response: Page 1 line 27, this mistake has been corrected.

3. Please homogenize the dry and wet period definition: in the introduction it says that the dry season extends from November to May; in section 2.1 it says that the dry season is from December to March; in section 2.3.1 it says that dry season is generally defined from November to April; in the same section 2.3.1 it is coherent within the section and it says that "Our study taking place from March to June allowed for the observation of both the late part of the dry season (March-April) and the beginning of the wet season (May-June)"; in the conclusions section it says "during four months of the 2015 dry season". Given that precipitation data for the specific campaign is available, according to section 2.2.3, could you please provide this data, or make the classification based on these data? (Although the info in literature about the usual dry-wet periods can still be included).

Author's response:
We understand our wording can be confusing. The two contrasted dry and wet seasons observed around the Equator originate from the closeness of the Intertropical Convergence Zone (ITCZ), which brings moist air masses and heavy precipitations. Kaly et al. (2015), based on 5 years of observations (2006-2010) at M'Bour, defined the dry season as the period during which no precipitation occurs from November to April and the wet season from May to October, where significant precipitation is measured, with a transition during April/May.
In Mortier et al. (2016), who analyzed data from 2006 to 2012 at M'Bour, the seasons are defined based on RH levels: from December to March/April (RH < 40%) for the dry season and from June to September (RH ~ 80%) for the wet season. They also observed different wind patterns at the ground level, that is to say trade winds coming mostly from the North-East during the dry season, whereas the wet season was characterized by winds from the west. During the AMMA field campaign in the Sahelian belt, Haywood et al. (2008) defined the period from May to June as the monsoon onset. Finally, Slingo et al. (2008) also mentioned "*large interannual variability in the seasonal progression of humidity, with no clearly reproducible pattern from year-to-year*" in Niamey, Niger.

Therefore we based the definition of the dry and wet seasons in this work on the observed weather parameters during the field campaign. Since absolutely no precipitation was observed during the whole period, but differences in RH levels (Figure R2) – though not as pronounced as reported by Mortier et al. (2016) – and wind patterns were clearly visible, we considered March and April to belong to the dry season and May-June to the transition period.

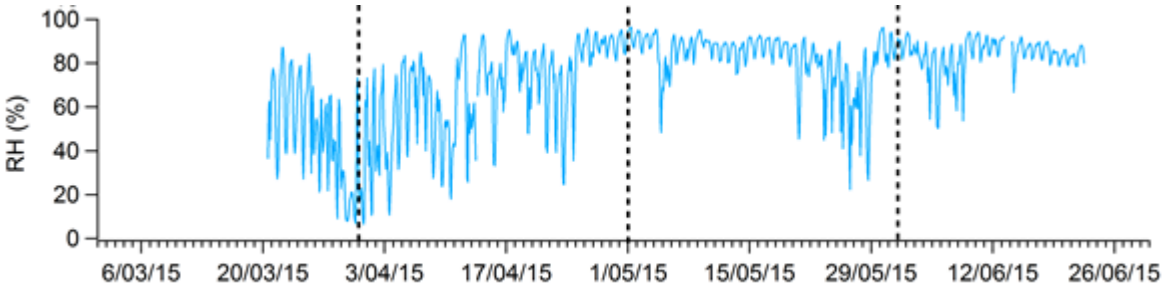

Figure R2. Time series of relative humidity (in %; 2-hour averages).

Changes in manuscript:

Complementary information concerning the distinction between dry and wet seasons has been added in section 2.3.1 "Classification of air masses", and some sentences have been simplified to hopefully make things clearer.

Page 2 lines 26-27, sentence modified: "During the months of January-February (dry season)"

Page 3 lines 30-31, sentence modified: "the dry season", with no mention of the month range.

Page 6 lines 16 - 24, paragraph modified: "The station of M'Bour is under the influence of a typical Sahelian climatic cycle composed of two contrasted dry and wet seasons observed around the Equator, which originate from the closeness of the Intertropical Convergence Zone (ITCZ), bringing moist air masses and heavy precipitations. Kaly et al. (2015), based on 5 years of observations (2006-2010) at M'Bour, defined the dry season as the period during which no precipitation occurs from November to April and the wet season from May to October, where significant precipitation is measured, with a transition during April/May. In Mortier et al. (2016), who analyzed data from 2006 to 2012 at M'Bour, the seasons are defined based on RH levels: from December to March/April (RH < 40%) for the dry season and from June to September (RH ~ 80%) for the wet season. They also observed different wind patterns at the ground level, that is to say trade winds coming mostly from the North-East during the dry season, whereas the wet season was characterized by winds from the west. During the AMMA field campaign in the Sahelian belt, Haywood et al. (2008) defined the period from May to June as the monsoon onset. Finally, Slingo et al. (2008) also mentioned large inter-annual variability in the seasonal progression of moisture, with no clearly reproducible pattern from year-to-year in Niamey, Niger.

Therefore we based the definition of the dry and wet seasons in this work on the observed weather parameters during the field campaign. Since absolutely no precipitation was observed during the whole period, but differences in RH levels – though not as pronounced as reported by Mortier et al. (2016) – and wind patterns were clearly visible (Figure 2a), we considered March (RH = 49%) and April (68%) to belong to the dry season, and May (82%) and June (84%) to the transition period."

4. Section 2.2.1. Please confirm that no major changes (such as filament replacement) occurred to the ACSM during the time between Feb 2014 and Jan 2015, for which the calibration constants were taken. This is necessary to be able to take the average of all calibrations. Especially between Dec 2014 and Jan 2015 there is a big difference for the RF of NO3 (Fig S1). This is a source of uncertainty that should be acknowledged in the manuscript, especially considering that the absolute concentrations are used and that the differences with the bulk PM1 concentrations are taken as very valid and interpreted.

Author's response:

We confirm that no major changes that could impact RF(NO_3) calibration occurred between Feb. 2014 and Jan. 2015. In particular, we have operated our ACSM with the same filament since its purchase in

2013. Additional calibrations performed since the end of the SHADOW field campaign have confirmed the stability of this value with an average of $(3.75 \pm 0.67) \times 10^{-11}$ Amps / (µg m^{-3}). It must be noted however that the uncertainties on mass concentrations with aerosol mass spectrometers are estimated at 20-35% (2σ) for the total mass (Bahreini et al., 2009). Furthermore, Crenn et al. (2015) reported reproducibility expanded uncertainties of Q-ACSM concentration measurements of 9, 15, 19, 28, and 36% for NR-PM_1, nitrate, organic matter, sulfate, and ammonium, respectively, during an intercomparison that involved 13 Q-ACSM in the Paris area during springtime.

Changes in the manuscript:
Page 5 lines 9 - 12, the text now reads: "It must be noted however that the uncertainties on mass concentrations with aerosol mass spectrometers are estimated at 20-35% (2σ) for the total mass (Bahreini et al., 2009). Furthermore, Crenn et al. (2015) reported reproducibility expanded uncertainties of Q-ACSM concentration measurements of 9, 15, 19, 28, and 36% for NR-PM_1, nitrate, organic matter, sulfate, and ammonium, respectively, during an intercomparison that involved 13 Q-ACSM in the Paris area during springtime."

5. Section 2.3.1. "During IOP-1 two main prevailing directions were found (Fig. 2a). The first one [...] and North-West to South-West (315-225_, dominant in May-June)"
Maybe you could indicate which wind direction prevails for the first and second periods (Mar-Apr and May-Jun), since the wind directions for the periods are given based on literature info, but the data for the specific campaign is available and then the wind roses are commented for the entire period.

Author's response:
The period from end of March to April was dominated by winds coming from NW to NE (~62%) with some occurrences (~33%) of Western winds during the sea breezes, while from May to June winds were mainly originating from the West (72%).

Changes in the manuscript:
Figure 2 has been modified to include wind frequency rose plots for March-April (dry season) and May-June (transition period). Besides, the following sentence has been added page 6, lines 30-31: "The period from end of March to April was dominated by winds coming from NW to NE (~62%) with some occurrences (~33%) of Western winds during the sea breezes, while from May to June winds were mainly originating from the West (72%)."

6. Section 2.3.1. "In summary, among the 91 days of IOP-1, 19% were classified as continental days, 32% as sea breeze days and 49% as marine days". You could say these percentages for the dry and wet periods? Or the rain for each of the 3 types of days? Somehow the info of the day types and the info on rain (dry-wet) should be linked. This is related to Fig 2 as well.

Author's response:
As indicated in reply to comment #3, no precipitation was observed during the whole campaign. Nonetheless, we provide in Table R3 below the number of days associated with the dry season (March-April) and the transition period (May-June).

Table R3. Number of days (relative contribution in parenthesis) associated with the continental, sea breeze and marine influences for the dry season, the transition period and the whole IOP-1.

	Continental	Sea breeze	Marine	Total
Mar-Apr.	13 (32%)	19 (48%)	8 (20%)	40 (100%)
May-Jun.	4 (8%)	10 (20%)	37 (73%)	51 (100%)
IOP-1	17 (19%)	29 (32%)	45 (49%)	91 (100%)

Changes in the manuscript:
Figure 2 in the manuscript now includes the wind roses for the dry season (March-April) and the transition period (May-June).

7. Section 3.1.1. "the fraction of unaccounted material therefore corresponded to DD and SS contributions". Note that if Fe is 2-5% of DD, then according to Fe concentrations, DD>unaccounted mass.

Author's response: As correctly pointed out in comment #1 by this reviewer and discussed in our reply, the Fe contribution to DD is 20% on average in PM_1, and not 2-5%.

8. Section 3.1.1. "The unaccounted fraction (determined as the difference between the gravimetrically measured PM_1 mass concentration and the sum of chemical species from ACSM and aethalometer measurements) corresponds to 27%, 26% and 16% of the PM1 mass for continental, sea breeze and marine days, respectively (see Figure S2)". Please specify that for these numbers you already applied the model from Fialho for this calculation, so that you derived already BC and Fe concentrations from the aethalometer measurements.

Changes in the manuscript:
Page 8 line 18, now added in the methodology section: "In the rest of the paper, when BC and Fe concentrations are mentioned, it corresponds to the deconvolved values based on the above-mentioned method."
Page 10 lines 4-7: "The unaccounted fraction was determined as the difference between the gravimetrically measured PM_1 mass concentration and the sum of chemical species from ACSM (Org, NO_3, SO_4, NH_4, Chl) and aethalometer (BC, Fe) measurements. It corresponded to 27%, 26% and 16% of the PM_1 mass for continental, sea breeze and marine days, respectively (see Figure S3)."

9. Section 3.1.1. Related with comment 4, please comment on the uncertainty of ACSM measurements since you took RF of NO3 as an average of previous calibrations and not determined on site.

Author's response:
Indeed we were not able to perform calibrations on site due to technical and regulatory constraints (for instance shipping our SMPS with a radioactive source to Senegal would have been nearly impossible). As indicated in the reply to comment #4, additional calibrations performed since the end of the SHADOW field campaign have confirmed the stability of the averaged value used for this campaign. Another (indirect) way to confirm that the calibrations are not too far off is the slope close to unity of Figure S4a that shows NH_4 measured vs. NH_4 predicted since these two parameters depend on both RF(NO3) and RIE values (at least of the main inorganic species that neutralize NH_4), as mentioned page 12 lines 32-34.

10. Section 3.1.2. "Although a weak correlation (r = 0.55) was found between Fe and total PM1 concentrations, Fe concentrations showed higher correlations with PM_{10} (r = 0.70, see Figure 4)". You could check the correlation between Fe and PM1-ACSM-BC.

Author's response: The correlation observed between Fe and the unaccounted PM_1 is even worse for the whole IOP-1 (r = 0.47). It is partly due to the absence of TEOM-FDMS PM_1 measurements during the periods with major dust events (whereas TEOM PM_{10} measurements were available), that leads to excluding Fe concentrations above 4 µg m^{-3}.

Changes in the manuscript:
Page 10 lines 32-35 now reads: "Although weak correlations were found between Fe and total PM_1 concentrations (r = 0.55) and unaccounted PM_1 (r = 0.47), Fe concentrations showed higher

correlations with PM_{10} (r = 0.70, see Figure 4). This could be explained by the lack of PM_1 mass concentration measurements during intense dust events, as well as DD domination in the coarse fraction, while the fine fraction is mainly driven by NR and BC species during most of the IOP-1 (Figure 3c)."

11. Section 3.1.2. "the highest Fe concentrations (> 8.0 µg m-3) are generally associated with continental and sea breeze days. These maxima also coincide with PM10 highest concentrations (> 400 µg m-3)". Note that 8 µg m-3 of Fe corresponds to 160 µg m-3 of DD (if Fe is 5% of DD on average according to literature values). Even if we assume a high percentage of refractory PM1 for this data point (higher than the average 29% according to data in page 9, line 24), let's estimate 60% of PM1 is refractory, this would mean that the PM1 is 267 _g m-3. If PM10 is 400 _g m-3, then the ratio PM1/PM10 for this event would be 67%, much higher than the average 10% reported.
Is this the case? Please check for consistency. Either Fe is overestimated, or PM1 is underestimated, or both.

Author's response: During the whole IOP-1, the PM_1/PM_{10} ratio average was indeed 10% but it varied between 2 and 55% for 2-hour averages. We expect it to be closer to the lower values during dust events (according to Figure 3b), for which unfortunately we had to invalidate PM_1 mass concentrations. Additionally, we recalculated the percentage of {Fe + Unacc.} in PM_1 for the highest PM_{10} concentrations (> 400 µg m^{-3}) and found an average value of 0.77 ± 0.04, slightly higher than the 60% used in the reviewer's calculations.
Therefore, using our corrected ratio of 20% of Fe in submicron DD (see comment 1), 8 µg m^{-3} of Fe corresponds to 40 µg m^{-3} of DD, 52 µg m^{-3} of PM_1 and a PM_1/PM_{10} ratio of 13%, consistent with the values presented in the manuscript. Note that this is an upper value since the concentrations of PM_{10} reached 950 µg m^{-3} at the site, while the highest Fe concentration was 11.2 µg m^{-3}.

12. Section 3.1.2. Last paragraph. "Fe contributions to PM10 estimated in M'Bour (average Fe/PM_{10} ratio of 0.51% over IOP-1 and 0.89% for continental days)". The Fe concentrations determined in this study correspond to PM1, since the aethalometer was equipped with a PM_1 inlet. If this is correct, then the authors are taking the Fe in PM_1 with respect to bulk PM_{10}, whereas the Fe concentration in PM_{10} corresponding to the Fe concentrations in PM1 determined in the present study would be much higher. Hence the comparisons with the ratios of Fe/DD or Fe/soil in the literature are not direct. Regarding the sentence "Nonetheless they (Formenti et al in PM_{40}) measured for the same samples an averaged iron concentration of 10 µg m^{-3}, in the same order of magnitude as our maximum concentration of 11.2 µg m^{-3} in PM_1"; this is not directly comparable, Fe in PM40 with Fe in PM_1.

Author's response: As mentioned in reply to comment 1 (Table 1), we only found one study that determined the iron content in PM_1 DD, leading to a value of 7.8% in the absence of dust events, which is within the same order of magnitude with the one found here, i.e. 20%.
We agree with reviewer #2 that our wording is confusing in this paragraph since the Fe/PM_{10} ratio refers indeed to Fe_{PM1} / PM_{10} and not to the proportion of Fe in the PM_{10} size fraction.
Direct comparisons with other size fractions cannot be straightforward since it would assume that the contribution of Fe is constant whatever the particle size, although literature has shown that, as mentioned above (comment 1), iron oxides belong mostly (for ~2/3) to the clay fraction (~$PM_{2.5}$) and ~1/3 to the silt (coarse) fraction (Journet et al., 2014; Kandler et al., 2009), which is consistent with increased ratios in the submicron fraction compared to larger ones.

Changes in the manuscript:
Page 11 lines 3-13: "From the only study in the literature focusing on iron concentrations in the submicron fraction in West Africa (Val et al., 2013), we could infer an elemental iron contribution of 7.8% to PM_1 dust, in Dakar, in the absence of dust events. Other studies focused on dust gave the iron contribution for size fractions higher than PM_1, thus no straightforward comparisons can be made with our average ratios of Fe/DD_{PM1} (20, 23, 21 and 16% for respectively IOP-1, continental, sea breeze

and marine days). It can nevertheless be interesting to have in mind values retrieved within the same region as it is known that iron oxides mainly belong to the finest fraction (Journet et al., 2014; Kandler et al., 2009) and therefore the elemental iron contribution should be lower for larger sizes, which is consistent with values reported in Table S2.2."

13. Section 3.1.2. To compare with % determined in DD or soil samples, the ratios that should be taken from this study are the Fe/(PM1-ACSM-BC), assuming PM1-ACSMBC a proxy for DD if we disregard sea salt, as DD or soil samples do not have the NR components that we have in the PM1 in this study. This ratio (Fe/(PM1-ACSM-BC)) is 20% approx for IOP-1 and about 23% for continental days (according to Figure S2).

Author's response: See response to comment 1.

14. Section 3.1.3. "regional background sites such as MontSec, Spain". Consider replacing regional by continental, since Montsec site is defined as continental back-ground site in Ripoll et al, 2015.

Changes in the manuscript:
Page 11 line 25: "continental background sites such as MontSec"

15. Section 3.1.4. The wind is always from the North (NW-NE), so the variation along the day cannot be explained by transport only, since the transport takes place the entire daytime (during the night the wind velocity is lower, so this can partially explain some variation).

Author's response: We agree with the reviewer that for continental days, the wind is always blowing from the NW to NE, whereas during sea breeze days, part of the afternoon is under the influence of marine air masses, and for marine days western winds dominate.
We have indeed highlighted several times in that section that for continental days the observed temporal variations are also coming from the temporal variability of local emissions.
For instance, page 13 lines 13-14: "*suggesting an influence linked to emissions by rather local anthropogenic activities rather than long-range transport sources*"; page 13, line 28: "*probably combining local emissions and reduced dispersion*"; page 13, lines 34-35: "*These peaks are measured for air masses coming from the continent and correspond to traffic and/or cooking hours*"; page 14, line 1: "*(…) tend to confirm combustion sources for these species*".

16. Section 3.2.2. "The HOA rose plot shows marked peaks in the directions of the two open waste burning areas and of the fish-smoking area located northeast of the site in the outskirts of M'Bour". Can you please give a tentative explanation for this?

Author's response: HOA rose plot and NWR plot both show higher concentrations in these directions. As for the open waste burning areas, a possible explanation could be the formation of organic compounds which present molecular structures that, when fragmented by electron impact ionization, are very similar to the HOA mass spectrum for m/z below 100. This is for instance the case for phthalate esters (Wienecke et al., 1992), whose mass spectrum is shown below.

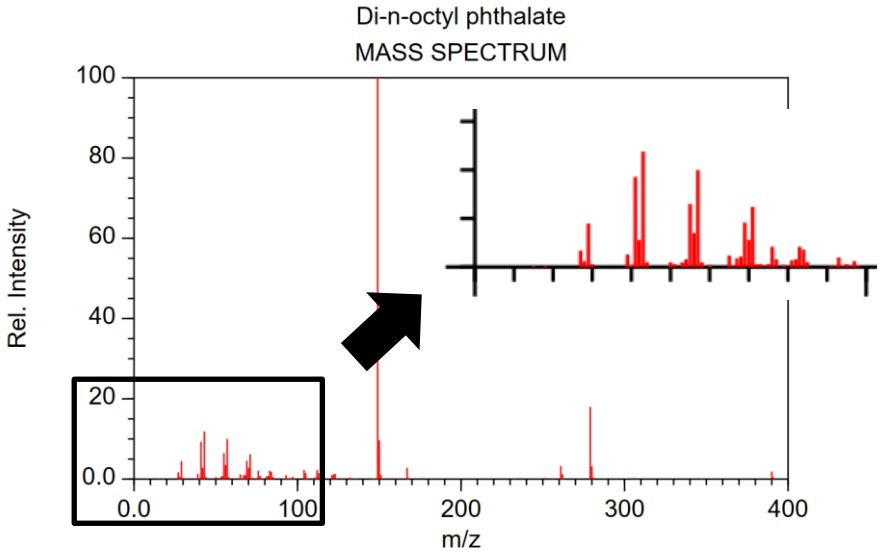

Figure R3. Mass spectrum of di-n-octyl phthalate obtained by electron impact ionization

It is less obvious why HOA points out also to the fish-smoking area. We have not been able to observe the process of fish-smoking but were told that they used millet flour as fuel. Since it is extracted from the grains, it should contain almost no cellulose (0.7-1.8% according to Wankhede et al. -1979)), contrary to the stems of plants where it amounts to ~40% (Ververis et al., 2004). This could explain why we do not see any biomass burning tracer, since levoglucosan is formed by the pyrolysis of cellulose. Finally, we cannot exclude higher traffic emissions at this location during the hours when the fish is smoked, since it has to be transported from the harbour to the fish-smoking area.

17. Section 3.2.2. Could you comment on the 5-factors solution constraining HOA and COA? Do you get LCOA and 2 different OOA factors? If this is the case, you could see different origins for OOA, ideally locally formed versus transported? Or is the 5-factors solution resulting in a mix LCOA-OOA factor not well defined?

Author's response: The 5-factor solution presented in Appendix S6 of the submitted manuscript (now Appendix S8) was obtained with m/z 36 in the PMF input in addition to the "classical" organics matrix. This mass was consistently attributed to the LCOA factor, as mentioned in the Appendix discussion. Besides, strong constraints on the different POA factors (using profiles of HOA, COA and LCOA obtained with unconstrained solutions) were applied. In these conditions only, two different kinds of OOA factors could be deconvolved: one more oxidized (MO-OOA; 76.5% of OOA) and considered from a more regional origin (mostly marine as highlighted by its NWR plot and PSCF map in Figure R4 below) and the other less oxidized (LO-OOA; 23.5% of OOA), locally emitted as per its NWR plot. Nonetheless, without using m/z 36 as input and literature profiles for constraining HOA and COA none of the solution leads to two completely distinct OOA profiles. If considering MO-OOA only, most of it could be rather due to the oxidation of ship emissions along the Western African coast, which would also explain the better correlation observed with NO_3 from NO_x emission processing despite the predominance of this regional oxidized factor over the local one.

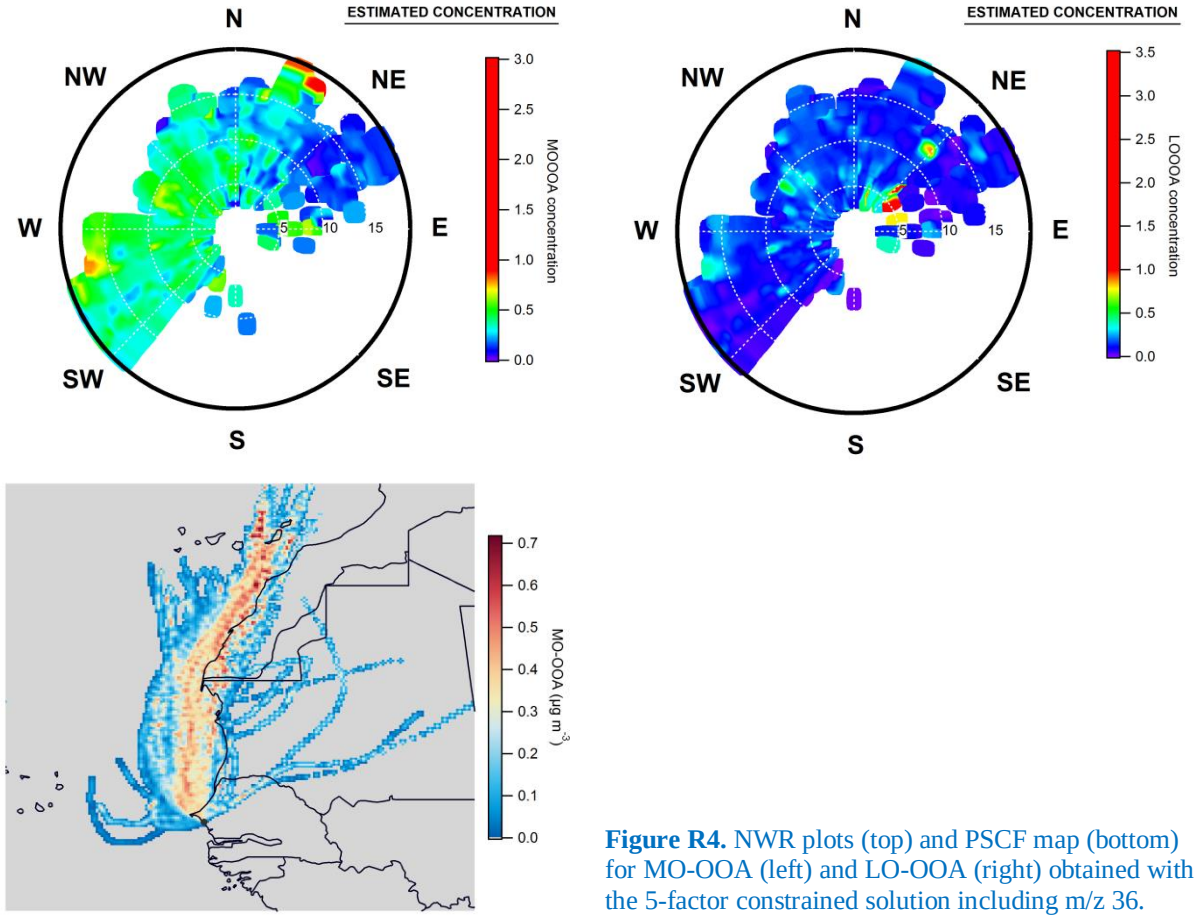

Figure R4. NWR plots (top) and PSCF map (bottom) for MO-OOA (left) and LO-OOA (right) obtained with the 5-factor constrained solution including m/z 36.

Changes in the manuscript:

Abstract, page 2 lines 4-6: "The remaining fraction was identified as oxygenated organic aerosols (OOA), a factor that prevailed regardless of the day type (45%) and was representative of regional (~3/4) but also local (~1/4) sources due to enhanced photochemical processes."

Page 15 lines 34-36: "Since the behavior of Chl had also been suspected to come from the same sources, PMF solutions adding the m/z 36 signal in the input matrix were investigated, and a solution is presented in Appendix S8, where regional OOA accounts for ~3/4 of the OOA and local OOA ~1/4."

Page 18 line 21: "The OOA PSCF map (Figure S5c) seems to trace back its origin along the entire Western African coast, where shipping emissions could be a major source of organic aerosols."

18. Section 3.2.2. The COA profile does not meet the 41>43 characteristic of the COA. Do you have any comment on this?

Author's response: HOA and COA profiles were quite difficult to separate over the whole period when running unconstrained PMF, as has been shown in previous studies with Q-ACSM (Fröhlich et al., 2015 and references therein). When applying strong constraints on the primary profile, part of the m/z 43 fragment goes to HOA and OOA, as observed in the 5-factor constrained solution (Appendix S8). However this does not change significantly the contribution of this factor to the total OA.

19. Section 3.2.2. “Our measurements over a large period of four months”. Please re-write to state the 3 months period. Maybe 3 months cannot be considered a large period (true it is larger than typical 3 weeks campaign for AMS, but it is not very large).

Changes in the manuscript:
Page 18 line 30: “over a period of three months”

20. Conclusions section. “during four months of the 2015 dry season”. Please revise if you wanted to say dry season, or dry+wet. Please correct the duration to 3 months.

Changes in the manuscript:
Page 18 lines 35-36: “during three months encompassing the end of the dry season and the transition period toward the wet season of 2015”

21. Conclusions section. “This factor (LCOA), although minor on average, could represent as high as 7% on a 30-minute time period when the air masses were blowing from the waste burning areas”. Isn’t it even more as a maximum? The average contribution of LCOA for marine events is 7%, so there must be some individual 30-min data points with a higher contribution. Or are these points you mention when air masses blow from the waste burning areas not taking place during marine-classified days? Maybe worth to clarify this. Moreover, maybe worth to clarify also the differences in absolute contributions, although the percentage is higher for marine days (by a factor of 2 or 3 with respect to other days), the absolute contribution is not so much higher. Still the absolute contribution for marine is higher (continental: 5.98 µg m^{-3} x 36% of OA x 2% of LCOA= 0.04 µg m^{-3} of LCOA; sea breeze: 6.29 µg m^{-3} x 40% of OA x 3% of LCOA=0.08 _g m-3 of LCOA; marine: 6.09 µg m^{-3} x 25% of OA x 7% of LCOA=0.11 µg m^{-3} of LCOA) (calculations to be improved with the corresponding decimals and not rounded values taken from the plots). Why the absolute average contribution of LCOA is higher for marine days even that during marine days the wind is never coming from the identified waste burning sources, according to map and wind rose in Figs 1 and 2?

Author’s response: Overall the concentration of LCOA is 0.05 (11%), 0.06 (17%) and 0.07 (34%) µg m^{-3} on average (maximum contribution) for continental, sea breeze and marine days, respectively. Days during which air masses were coming from the identified open waste burning areas of Gandigal or/and Saly Douté were classified either as continental or sea-breeze days. Some strong events also appear during marine days at an average distance from the site (see LCOA NWR plot in Figure S5b) and may be related to air masses carried over Dakar where similar massive anthropogenic emissions from waste burning could be expected from Mbeubeuss, the largest dumpsite in Senegal located 25 km north-east of Dakar along the coast, which receives 250,000 tons of garbage per year from the Dakar region (Cissé, 2012). In the absence of strictly controlled waste regulations, it is however quite likely there are other unidentified open waste burning sites along the coast that could also contribute to this factor. The more regional influence seen in the NWR plot may also be due to chlorine-driven photo-oxidation processes occurring off the coast of Senegal (Hossaini et al., 2016).

Changes in the manuscript: The dumpsite of Mbeubeuss in Dakar is now identified in Figure 1.

Page 17 line 29: “Besides, the NWR plots of Chl (local influence) and LCOA (both local and regional) rather suggest the presence of chlorinated organics. The PSCF maps identify two possible origins, one clearly from the ocean that could be related to chlorine-driven photo-oxidation processes (Hossaini et al., 2016) and the other linked to air masses carried over Dakar where similar massive anthropogenic emissions from waste burning could be expected from Mbeubeuss, the largest dumpsite in Senegal located 25 km north-east of Dakar along the coast, which receives 250,000 tons of garbage per year from the Dakar region (Cissé, 2012).

Page 19 lines 19-26: “Three primary OA linked to anthropogenic activities from nearby sources were also identified: HOA (22%), COA (28%) and a new factor LCOA (3%) related to local combustion sources (emissions from open-waste burning and fish smoking areas), for which a good correlation with particulate chloride (m/z 36) was consistently found. Non-refractory chloride fragments from waste burning or fish smoking areas were suggested to originate from local plastic smoldering/flaming processes (for the former) and/or sea salt (for both) submitted to high temperatures under continental influence. This factor, although minor on average, could represent as high as 7% on a 30-minute time period when the air masses were blowing from the local waste burning areas, and very likely resulted in the concomitant emissions of highly-toxic compounds such as dioxins that would require further investigation. Back-trajectories also suggest possible distant sources of combustion, with part of LCOA, OOA and BC associated to processed oceanic air masses which could be influenced by Dakar traffic emissions and waste burning activities, as well as shipping emissions along the West African coast.”

22. Figure 5. Maybe choose a different color for Fe (in print it looks same as sulfate).

Changes in the manuscript: Figure 5 has been modified as suggested using dark brown for iron.

23. Figure 7a. Consider choosing a different scale for OM and (SO4, NH4, NO3 and Chl) to help seeing the variations, not very evident now for components different from OM.

Changes in the manuscript: Figure 7a has been modified as suggested, plotting OM on the right axis and all the other concentrations on the left one.

24. Figure 7b. Fe correlates with BC. This is an indication that the Fe calculation should be revised. The explanation of the co-transport of BC and Fe may not explain completely this parallel behavior. You could isolate the dust events and see the differences in Fe and BC ratios.

Author’s response: A correlation coefficient of 0.55 between Fe and BC was calculated for the whole IOP-1. Both species show quite distinctive origins (Figure S5b and S5c), iron sources pointing toward the Saharan desert (PSCF map) but also attributed to more local emissions most probably caused by traffic resuspension (NWR plot). BC appeared to be emitted both by cities located along the Western African coast especially Dakar (PSCF) and by local sources and attributable to diesel combustion from traffic which could explain the common peaks encountered in the morning and the evening by the two compounds.

25. Figure S6. Should legend in first plot read LCOA instead of WCOA?

Changes in the manuscript: The legend of Figure S8 (formerly Fig. S6) has been corrected.

References cited in this reply

Bahreini, R., Ervens, B., Middlebrook, A. M., Warneke, C., de Gouw, J. A., DeCarlo, P. F., Jimenez, J. L., Brock, C. A., Neuman, J. A., Ryerson, T. B., Stark, H., Atlas, E., Brioude, J., Fried, A., Holloway, J. S., Peischl, J., Richter, D., Walega, J., Weibring, P., Wollny, A. G. and Fehsenfeld, F. C.: Organic aerosol formation in urban and industrial plumes near Houston and Dallas, Texas, J. Geophys. Res. Atmospheres, 114(D7), D00F16, doi:10.1029/2008JD011493, 2009.

Caponi, L., Formenti, P., Massabó, D., Di Biagio, C., Cazaunau, M., Pangui, E., Chevaillier, S., Landrot, G., Andreae, M. O., Kandler, K., Piketh, S., Saeed, T., Seibert, D., Williams, E., Balkanski, Y., Prati, P. and Doussin, J.-F.: Spectral- and size-resolved mass absorption efficiency of mineral dust

aerosols in the shortwave: a simulation chamber study, Atmos Chem Phys Discuss, 2017, 1–39, doi:10.5194/acp-2017-5, 2017.

Cissé, O.: Les décharges d'ordures en Afrique - Mbeubeuss à Dakar au Sénégal, Karthala., 2012.

Crenn, V., Sciare, J., Croteau, P. L., Verlhac, S., Fröhlich, R., Belis, C. A., Aas, W., Äijälä, M., Alastuey, A., Artiñano, B., Baisnée, D., Bonnaire, N., Bressi, M., Canagaratna, M., Canonaco, F., Carbone, C., Cavalli, F., Coz, E., Cubison, M. J., Esser-Gietl, J. K., Green, D. C., Gros, V., Heikkinen, L., Herrmann, H., Lunder, C., Minguillón, M. C., Močnik, G., O'Dowd, C. D., Ovadnevaite, J., Petit, J.-E., Petralia, E., Poulain, L., Priestman, M., Riffault, V., Ripoll, A., Sarda-Estève, R., Slowik, J. G., Setyan, A., Wiedensohler, A., Baltensperger, U., Prévôt, A. S. H., Jayne, J. T. and Favez, O.: ACTRIS ACSM intercomparison – Part 1: Reproducibility of concentration and fragment results from 13 individual Quadrupole Aerosol Chemical Speciation Monitors (Q-ACSM) and consistency with co-located instruments, Atmos Meas Tech, 8(12), 5063–5087, doi:10.5194/amt-8-5063-2015, 2015.

Fialho, P., Freitas, M. C., Barata, F., Vieira, B., Hansen, A. D. A. and Honrath, R. E.: The Aethalometer calibration and determination of iron concentration in dust aerosols, J. Aerosol Sci., 37(11), 1497–1506, doi:10.1016/j.jaerosci.2006.03.002, 2006.

Formenti, P., Rajot, J. L., Desboeufs, K., Caquineau, S., Chevaillier, S., Nava, S., Gaudichet, A., Journet, E., Triquet, S., Alfaro, S., Chiari, M., Haywood, J., Coe, H. and Highwood, E.: Regional variability of the composition of mineral dust from western Africa: Results from the AMMA SOP0/DABEX and DODO field campaigns, J. Geophys. Res. Atmospheres, 113(D23), D00C13, doi:10.1029/2008JD009903, 2008.

Fröhlich, R., Crenn, V., Setyan, A., Belis, C. A., Canonaco, F., Favez, O., Riffault, V., Slowik, J. G., Aas, W., Aijälä, M., Alastuey, A., Artiñano, B., Bonnaire, N., Bozzetti, C., Bressi, M., Carbone, C., Coz, E., Croteau, P. L., Cubison, M. J., Esser-Gietl, J. K., Green, D. C., Gros, V., Heikkinen, L., Herrmann, H., Jayne, J. T., Lunder, C. R., Minguillón, M. C., Močnik, G., O'Dowd, C. D., Ovadnevaite, J., Petralia, E., Poulain, L., Priestman, M., Ripoll, A., Sarda-Estève, R., Wiedensohler, A., Baltensperger, U., Sciare, J. and Prévôt, A. S. H.: ACTRIS ACSM intercomparison – Part 2: Intercomparison of ME-2 organic source apportionment results from 15 individual, co-located aerosol mass spectrometers, Atmos Meas Tech, 8(6), 2555–2576, doi:10.5194/amt-8-2555-2015, 2015.

Hansen, A. D. A.: Aethalometer Operations Manual, Magee scientifique, Berkeley, CA, USA., 2005.

Haywood, J. M., Pelon, J., Formenti, P., Bharmal, N., Brooks, M., Capes, G., Chazette, P., Chou, C., Christopher, S., Coe, H., Cuesta, J., Derimian, Y., Desboeufs, K., Greed, G., Harrison, M., Heese, B., Highwood, E. J., Johnson, B., Mallet, M., Marticorena, B., Marsham, J., Milton, S., Myhre, G., Osborne, S. R., Parker, D. J., Rajot, J.-L., Schulz, M., Slingo, A., Tanré, D. and Tulet, P.: Overview of the Dust and Biomass-burning Experiment and African Monsoon Multidisciplinary Analysis Special Observing Period-0, J. Geophys. Res. Atmospheres 1984–2012, 113(D23), doi:10.1029/2008JD010077, 2008.

Hossaini, R., Chipperfield, M. P., Saiz-Lopez, A., Fernandez, R., Monks, S., Feng, W., Brauer, P. and von Glasow, R.: A global model of tropospheric chlorine chemistry: Organic versus inorganic sources and impact on methane oxidation, J. Geophys. Res. Atmospheres, 121(23), 2016JD025756, doi:10.1002/2016JD025756, 2016.

Joshi, N., Romanias, M., Riffault, V. and Thévenet, F.: Investigating water adsorption on natural mineral dust particles: A DRIFT and BET theory study, under press, Aeolian Research, 2017.

Journet, E., Balkanski, Y. and Harrison, S. P.: A new data set of soil mineralogy for dust-cycle modeling, Atmos Chem Phys, 14(8), 3801–3816, doi:10.5194/acp-14-3801-2014, 2014.

Kaly, F., Marticorena, B., Chatenet, B., Rajot, J. L., Janicot, S., Niang, A., Yahi, H., Thiria, S., Maman, A., Zakou, A., Coulibaly, B. S., Coulibaly, M., Koné, I., Traoré, S., Diallo, A. and Ndiaye, T.: Variability of mineral dust concentrations over West Africa monitored by the Sahelian Dust Transect, Atmospheric Res., 164–165, 226–241, doi:10.1016/j.atmosres.2015.05.011, 2015.

Kandler, K., SchÜTz, L., Deutscher, C., Ebert, M., Hofmann, H., JÄCkel, S., Jaenicke, R., Knippertz, P., Lieke, K., Massling, A., Petzold, A., Schladitz, A., Weinzierl, B., Wiedensohler, A., Zorn, S. and Weinbruch, S.: Size distribution, mass concentration, chemical and mineralogical composition and derived optical parameters of the boundary layer aerosol at Tinfou, Morocco, during SAMUM 2006, Tellus B, 61(1), 32–50, doi:10.1111/j.1600-0889.2008.00385.x, 2009.

Lafon, S., Rajot, J.-L., Alfaro, S. C. and Gaudichet, A.: Quantification of iron oxides in desert aerosol, Atmos. Environ., 38(8), 1211–1218, doi:10.1016/j.atmosenv.2003.11.006, 2004.

Lafon, S., Sokolik, I. N., Rajot, J. L., Caquineau, S. and Gaudichet, A.: Characterization of iron oxides in mineral dust aerosols: Implications for light absorption, J. Geophys. Res. Atmospheres, 111(D21), D21207, doi:10.1029/2005JD007016, 2006.

Linke, C., Möhler, O., Veres, A., Mohácsi, Á., Bozóki, Z., Szabó, G. and Schnaiter, M.: Optical properties and mineralogical composition of different Saharan mineral dust samples: a laboratory study, Atmos Chem Phys, 6(11), 3315–3323, doi:10.5194/acp-6-3315-2006, 2006.

Moreno, T., Querol, X., Castillo, S., Alastuey, A., Cuevas, E., Herrmann, L., Mounkaila, M., Elvira, J. and Gibbons, W.: Geochemical variations in aeolian mineral particles from the Sahara–Sahel Dust Corridor, Chemosphere, 65(2), 261–270, doi:10.1016/j.chemosphere.2006.02.052, 2006.

Mortier, A., Goloub, P., Derimian, Y., Tanré, D., Podvin, T., Blarel, L., Deroo, C., Marticorena, B., Diallo, A. and Ndiaye, T.: Climatology of aerosol properties and clear-sky shortwave radiative effects using Lidar and Sun photometer observations in the Dakar site, J. Geophys. Res. Atmospheres, 121(11), 2015JD024588, doi:10.1002/2015JD024588, 2016.

Müller, T., Schladitz, A., Massling, A., Kaaden, N., Kandler, K. and Wiedensohler, A.: Spectral absorption coefficients and imaginary parts of refractive indices of Saharan dust during SAMUM-1, Tellus B, 61(1), 79–95, doi:10.1111/j.1600-0889.2008.00399.x, 2009.

Petzold, A., Rasp, K., Weinzierl, B., Esselborn, M., Hamburger, T., Dörnbrack, A., Kandler, K., Schütz, L., Knippertz, P., Fiebig, M. and Virkkula, A.: Saharan dust absorption and refractive index from aircraft-based observations during SAMUM 2006, Tellus B, 61(1), 118–130, doi:10.1111/j.1600-0889.2008.00383.x, 2009.

Schladitz, A., Müller, T., Kaaden, N., Massling, A., Kandler, K., Ebert, M., Weinbruch, S., Deutscher, C. and Wiedensohler, A.: In situ measurements of optical properties at Tinfou (Morocco) during the Saharan Mineral Dust Experiment SAMUM 2006, Tellus B, 61(1), 64–78, doi:10.1111/j.1600-0889.2008.00397.x, 2009.

Slingo, A., Bharmal, N. A., Robinson, G. J., Settle, J. J., Allan, R. P., White, H. E., Lamb, P. J., Lélé, M. I., Turner, D. D., McFarlane, S., Kassianov, E., Barnard, J., Flynn, C. and Miller, M.: Overview of observations from the RADAGAST experiment in Niamey, Niger: Meteorology and thermodynamic variables, J. Geophys. Res. Atmospheres, 113(D13), D00E01, doi:10.1029/2008JD009909, 2008.

Val, S., Liousse, C., Doumbia, E. H. T., Galy-Lacaux, C., Cachier, H., Marchand, N., Badel, A., Gardrat, E., Sylvestre, A. and Baeza-Squiban, A.: Physico-chemical characterization of African urban aerosols (Bamako in Mali and Dakar in Senegal) and their toxic effects in human bronchial epithelial cells: description of a worrying situation, Part Fibre Toxicol, 10(10), 2013.

Ververis, C., Georghiou, K., Christodoulakis, N., Santas, P. and Santas, R.: Fiber dimensions, lignin and cellulose content of various plant materials and their suitability for paper production, Ind. Crops Prod., 19(3), 245–254, doi:10.1016/j.indcrop.2003.10.006, 2004.

Wankhede, D. B., Shehnaj, A. and Rao, M. R. R.: Carbohydrate composition of finger millet (Eleusine coracana) and foxtail millet (Setaria italica), Qual. Plant., 28(4), 293–303, doi:10.1007/BF01095511, 1979.

Wienecke, J., Kruse, H. and Wassermann, O.: Organic compounds in the waste gasification and combustion process, Chemosphere, 25(4), 437–447, doi:10.1016/0045-6535(92)90277-X, 1992.

Zotter, P., Herich, H., Gysel, M., El-Haddad, I., Zhang, Y., Močnik, G., Hüglin, C., Baltensperger, U., Szidat, S. and Prévôt, A. S. H.: Evaluation of the absorption Ångström exponents for traffic and wood burning in the Aethalometer-based source apportionment using radiocarbon measurements of ambient aerosol, Atmos Chem Phys, 17(6), 4229–4249, doi:10.5194/acp-17-4229-2017, 2017.